

A metallo pro-drug to target Cu(II) in the context of Alzheimer's disease

Amandine Conte-Daban,^[a,b] Vinita Ambike,^[c] Régis Guillot,^[c] Nicolas Delsuc,^[c,d] Clotilde Policar*^[c,d]
and Christelle Hureau*^[a,b]

[a] CNRS, LCC (Laboratoire de Chimie de Coordination), 205 route de Narbonne, BP 44099 31077 Toulouse Cedex 4, France

[b] Université de Toulouse, UPS, INPT, 31077 Toulouse Cedex 4, France

[c] Laboratoire des Biomolécules, Département de chimie, École normale supérieure, UPMC Univ. Paris 06, CNRS, PSL Research University, 24 rue Lhomond, 75005 Paris, France

[d] Sorbonne Universités, UPMC Univ. Paris 06, École normale supérieure, CNRS, Laboratoire des Biomolécules (LBM), 75005 Paris, France

[e] Institut de Chimie Moléculaire et des Matériaux d'Orsay, UMR CNRS 8182, Bâtiments 420, Université Paris-Sud 11, Université Paris-Saclay, Rue du doyen Georges Poitou, 91405 Orsay cedex, France.

E-mail : christelle.hureau@lcc-toulouse.fr; clotilde.policar@ens.fr.

Table S1. Crystallographic data and structure refinement details.

Compound	[Cu(LH)](PF ₆)(NO ₃)
Empirical Formula	C ₁₉ H ₂₆ Cu N ₆ O ₆ F ₆ P ₃ N O ₃
M_r	624.98
Crystal size, mm ³	0.32 x 0.21 x 0.06
Crystal system	triclinic
Space group	<i>P</i> - <i>1</i>
a, Å	8.8059(15)
b, Å	8.9439(17)
c, Å	15.920(3)
α , °	83.669(4)
β , °	78.476(4)
γ , °	88.162(4)
Cell volume, Å ³	1221.0(4)
Z ; Z'	2 ; 1
T, K	100(1)
Radiation type ; wavelength Å	MoK α ; 0.71073
F ₀₀₀	638
μ , mm ⁻¹	1.048
θ range, °	2.291 - 36.210
Reflection collected	21 222
Reflections unique	9 330
R _{int}	0.0312
GOF	1.100
Refl. obs. ($I > 2\sigma(I)$)	6 975
Parameters	342
wR ₂ (all data)	0.1658
R value ($I > 2\sigma(I)$)	0.0615
Largest diff. peak and hole (e ⁻ .Å ⁻³)	1.791 ; -1.318

Table S2. Selected bond distances (Å) and angles (°) for [Cu(LH)]²⁺.

Cu-N1	1.963(2)	Cu-N2	1.973(2)
Cu-N3	2.011(3)	Cu-N4	2.046(2)
Cu-O1	2.378(2)		
N1-Cu-N2	107.52(10)	N1-Cu-N3	82.68(11)
N1-Cu-N4	163.02(10)	N1-Cu-O1	102.37(9)
N2-Cu-N3	167.08(10)	N2-Cu-N4	84.09(9)
N2-Cu-O1	93.03(9)	N3-Cu-N4	84.31(10)
N3-Cu-O1	92.42(10)	N4-Cu-O1	89.01(9)

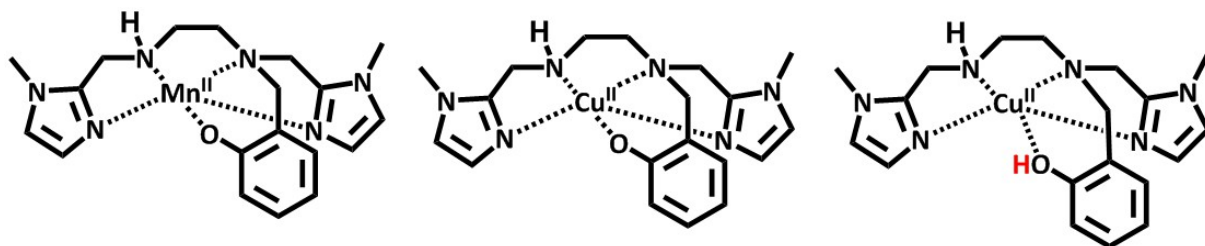


Figure S1. Scheme of 1⁺, 2⁺ and 2H²⁺.

EPR monitoring of metal swap between 1^+ and Cu(A β)

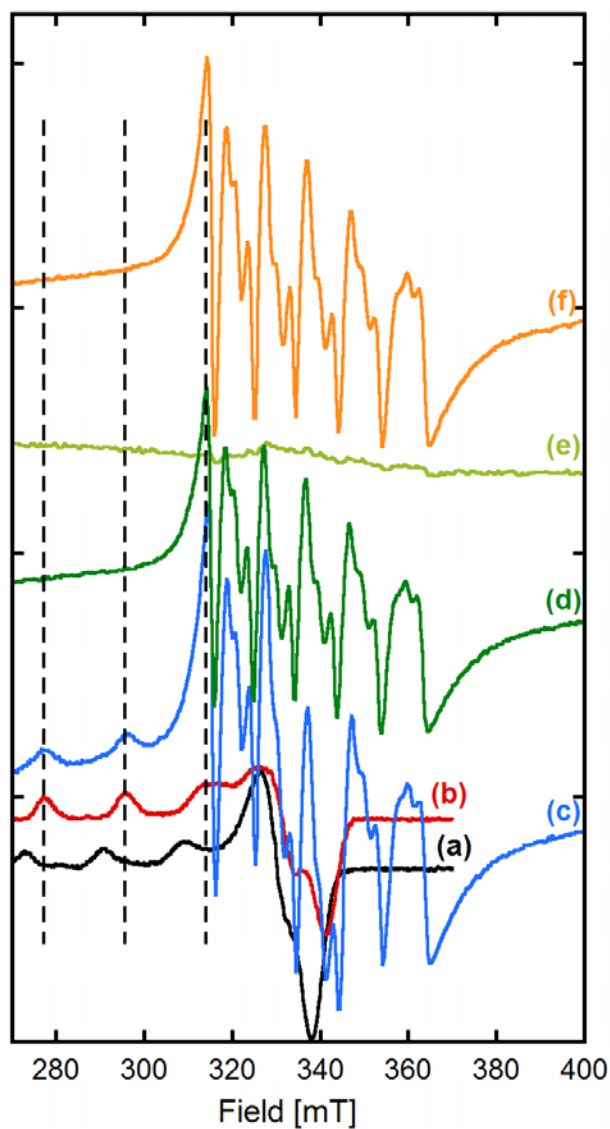


Figure S2. ^{65}Cu EPR signatures. *Panel A.* a) Cu(A β 16), b) 2^+ , c) Cu(A β 16) + 1^+ , d) Mn(A β 16), e) 1^+ , f) Mn(II) in buffer. $[^{65}\text{Cu}] = [\text{Mn(II)}] = 180 \mu\text{M}$, $[\text{A}\beta 16] = [\text{LH}] = [1^+] = 200 \mu\text{M}$, $[\text{HEPES}] = 50 \text{ mM}$, $\text{pH} = 7.1$. 10% of glycerol was used as a cryoprotectant. $T = 110 \text{ K}$, 0.5 mT of modulation amplitude, under non saturating conditions.

EPR monitoring of removal of Cu(II) from A β by LH

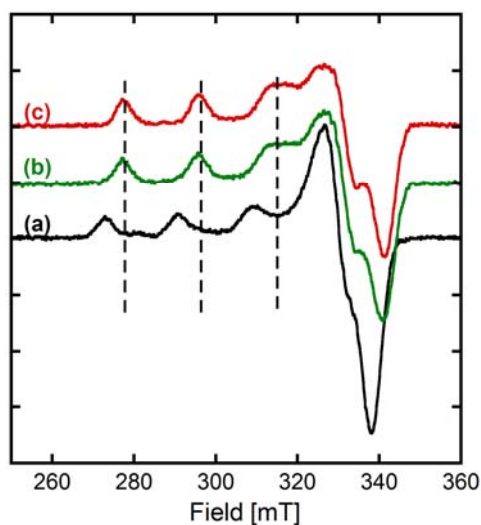


Figure S3. EPR signatures of a) Cu(A β 16), b) Cu(A β 16) + LH, c) $\underline{2}^+$. [^{65}Cu] = 180 μM , [A β 16] = [LH] = 200 μM , [hepes] = 50 mM, pH = 7.1. 10% of glycerol was used as a cryoprotectant.

UV monitoring of metal swap between $\underline{1}^+$ and Cu(A β)

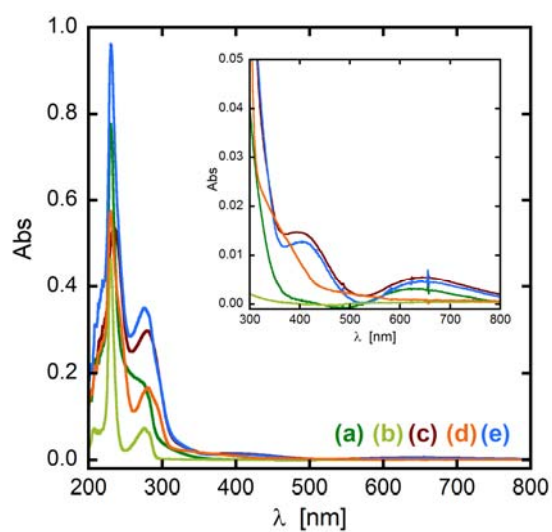


Figure S4. UV-Vis signature of a) Cu(A β 16), b) Mn(A β 16), c) $\underline{2}^+$, d) $\underline{1}^+$, e) Cu(A β 16) + $\underline{1}^+$. [LH] = [A β 16] = [Mn(II)] = [Cu(II)] = 50 μM , [HEPES] = 100 mM, pH = 7.1.

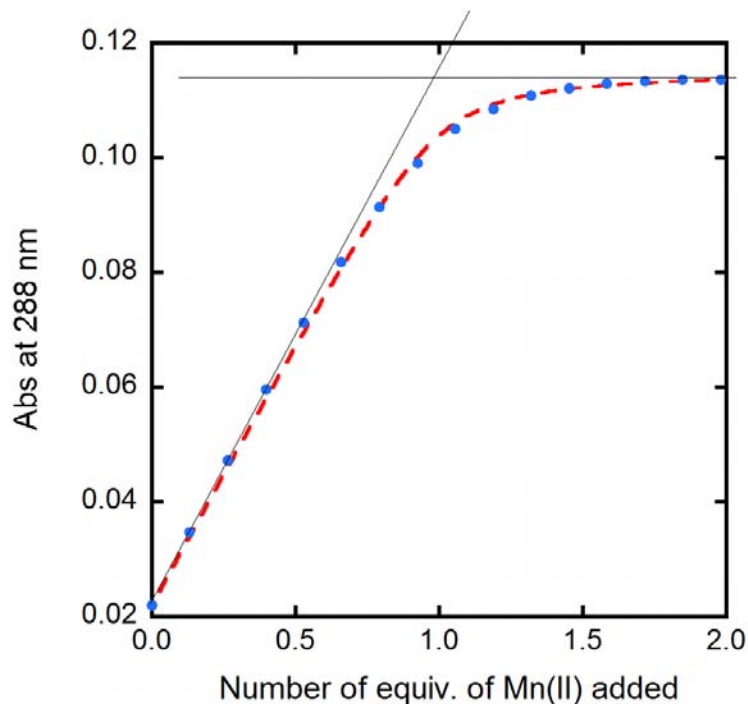


Figure S5. Determination by UV-Vis spectroscopy of the affinity constant at pH 7.1 of Mn(II) for LH. The absorbance at 288 nm with a subtraction at 320 nm is plotted as a function of the number of equiv. Mn(II) added. [LH] = 45 μM , [HEPES] = 100 mM, pH = 7.1. Red line: simulation of the experimental data with an affinity value of $1.3 \cdot 10^6 \text{ M}^{-1}$.

Determination of the affinity constants of Cu(II) for LH

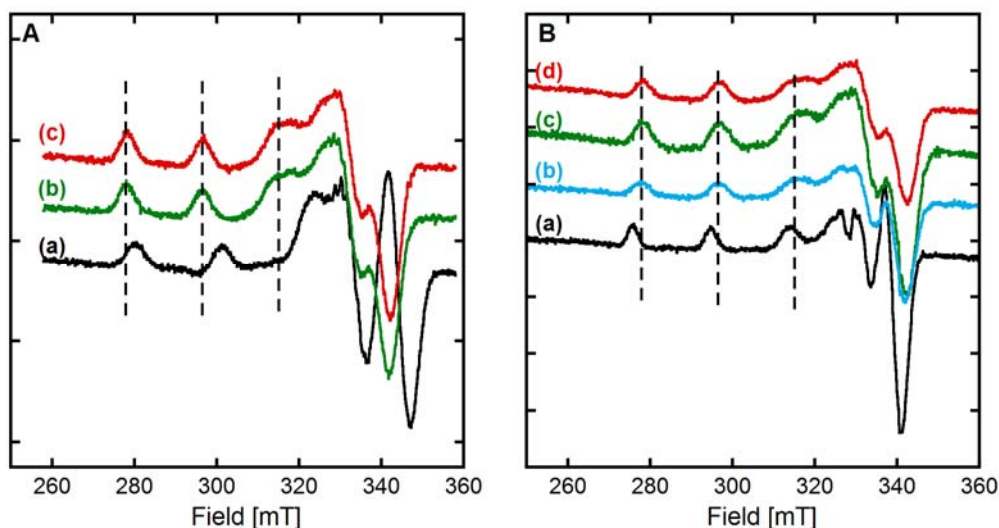


Figure S6. Competition experiments monitored by EPR between LH and competitors of known affinity to determine the affinity constant of Cu(II) for LH. *Panel A.* (a) Cu(DAHK), (b) 2^+ + 1 equiv. DAHK, (c) 2^+ . *Panel B.* (a) Cu(L₂), (b) 2^+ + 10 equiv. L₂, (c) 2^+ + 1 equiv. L₂, (d) 2^+ . [⁶⁵Cu] = 180 μM , [LH] = 200 μM , [HEPES] = 50 mM, pH = 7.1. 10% of glycerol was used as a cryoprotectant. Measured after equilibration of the reaction.

From the competition experiments shown above, it can be evaluated that the affinity of Cu(II) for LH is higher than that for DAHK (affinity of about 10^{13} M^{-1}) and at least 10 times greater than for L₂.

Comparison between spectra (a), (b) and (d) in panel B of Figure S4 show that at least 70% of the Cu(II) is bound to LH. An minimum affinity value of about 10^{16} M^{-1} is thus evaluated since at this pH L_2 has a conditional affinity constant of $10^{13.8} \text{ M}^{-1}$.^[1]

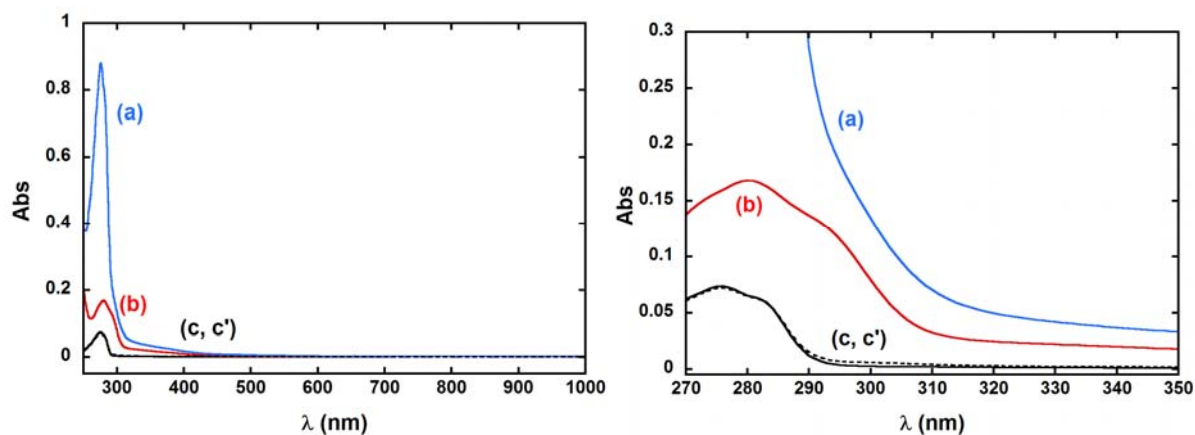


Figure S7. Competition experiments monitored by UV-Vis between $\mathbf{1}^+$ and A β 16. (a) $\mathbf{1}^+$ + 10 equiv. A β 16, (b) $\mathbf{1}^+$, (c) A β 16 (solid line) and (c') (spectrum (a) – spectrum (b)) /10 (dotted line). [LH] = 50 μM , [Mn(II)] = 45 μM , [HEPES] = 100 mM, pH = 7.1.

Calculated spectrum corresponding to (spectrum ($\mathbf{1}^+$ + 10 equiv. A β 16) – spectrum ($\mathbf{1}^+$)) /10 matches the UV-Vis signature of the A β 16 peptide, in line with the absence of significant removal of Mn(II) from $\mathbf{1}^+$ in presence of A β 16.

Mn(II) affinity values of multidentate imidazole and carboxylate-based synthetic

Table S3. Binding constants for the equilibrium Mn(II)/L (1/1).

For the original table and references therein, see ^[2].

Ligand	denticity	logK (T(°C)/ ionic strenght)	
Pyridine	monodentate	0.14 (25/0.5)	
Acetic acid		0.8 (25/0.16)	
2-aminomethyl-6-methyl-pyridine	bidentate	1.95 (25/0.1)	
D-tartric acid		2.49 (25/0.1)	
L-2-aminopropanoic acid (L-alanine)		2.5 (25/0.1)	
diglycolic acid		2.53 (25/0.1)	
2,2'-bipyridine		2.62 (25/0.1)	
2-aminomethyl-pyridine		2.66 (20/0.1)	
ethylenediamine		2.67 (25/0.1)	
phtalic acid		2.74 (25/0)	
aminoacetic acid (glycine)		2.8 (25/0.1)	
4-(2-aminoethyl)imidazole (histamine)		3.0 (25/0.2)	
1,10-phenanthroline		4.0 (25/0.1)	
diethylenetriamine		tridentate	3.99 (30/0.1)
di[2-picolyl]amine (DPA)			4.16 (25/0.1)
2,2',2''-terpyridine	4.4 (25/0.002-0.1)		
oxy-bis-propanedioic acid	tetradentate	4.51 (25/0.1)	
triethylenetetramine		4.9 (25/0.1)	
<i>N,N</i> -bis[(1-methylimidazol-2-yl)methyl]glycinate		5.3 (25/0.13)	
tris(2-picolyl)amine (TPA)		5.6 (20/0.1)	
tris(2-aminoethyl)amine (TREN)		5.8 (25/0.1)	
<i>N</i> -(2-carboxyphenyl)iminodiacetic acid		5.85 (25/0.1)	
<i>N,N'</i> -di(2-picolyl)ethylenediamine		5.9 (25/0.1)	
<i>N</i> -[(1-methyl-imidazol-2-yl)methyl]- <i>N</i> -(2-pyridylmethyl)glycinate (IPG)		6.0 (25/0.13)	
<i>N,N,N',N'</i> -(2-aminoethyl)ethylene diamine		hexadentate	9.26 (25/0.1)
<i>N,N,N',N'</i> -tetra-2-picolylethylenediamine (TPEN)			10.3 (20/0.1)

Determination of the pKa

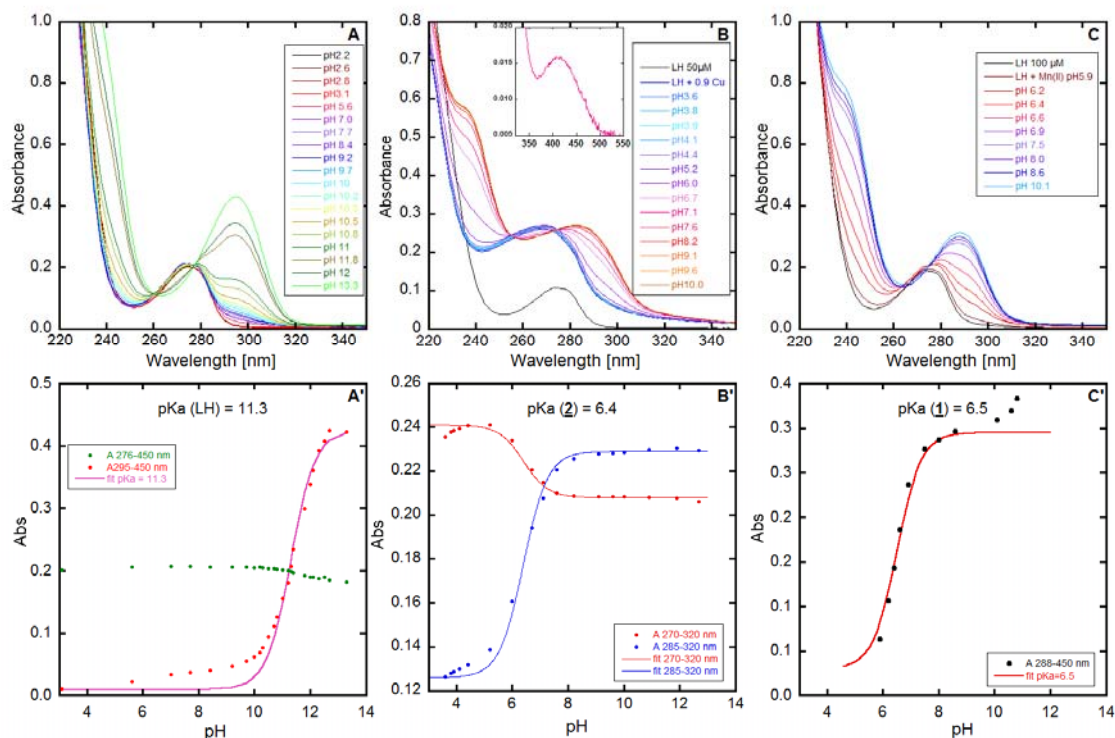


Figure S8. Determination by UV-visible spectroscopy of the pKa of LH (Panels A and A'), $\underline{2}^+$ (Panels B and B'), $\underline{1}^+$ (Panels C and C'). A) [LH] = 91 μM, B) [LH] = 45.6 μM, [Cu] = 45 μM, C) [LH] = 91 μM, [Mn] = 90 μM, T = 25°C. Inset in panel B shows a zoom on the 320-550 nm region of $\underline{2}^+$ at pH 7.1.

Deprotonation of phenol arm of LH is observed by the appearance of a UV-Vis band at 290 nm. Intensity of this band was plotted as a function of pH to determine the pKa values of the phenol group in LH, $\underline{1}^+$ and $\underline{2}^+$.

Cyclic voltammetry of 2.

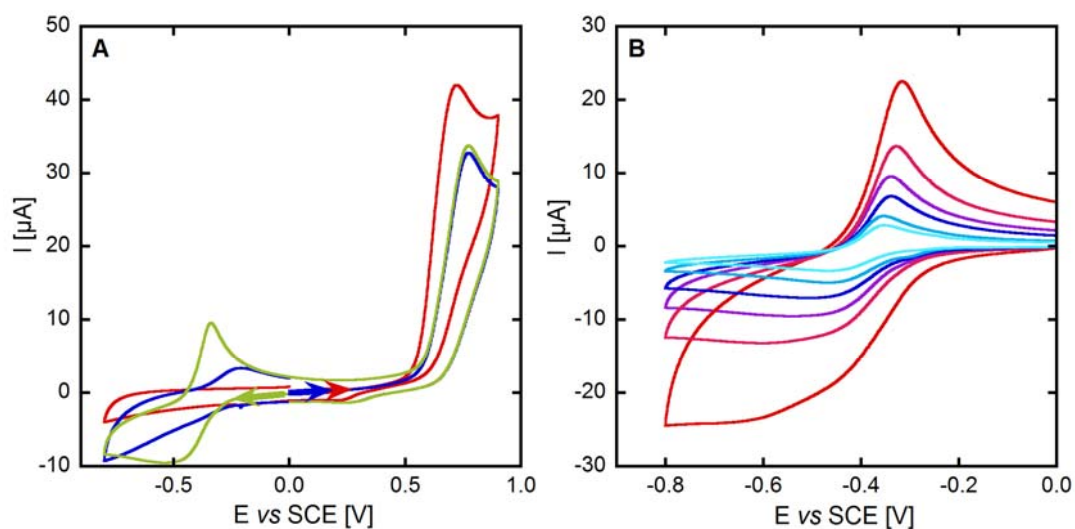
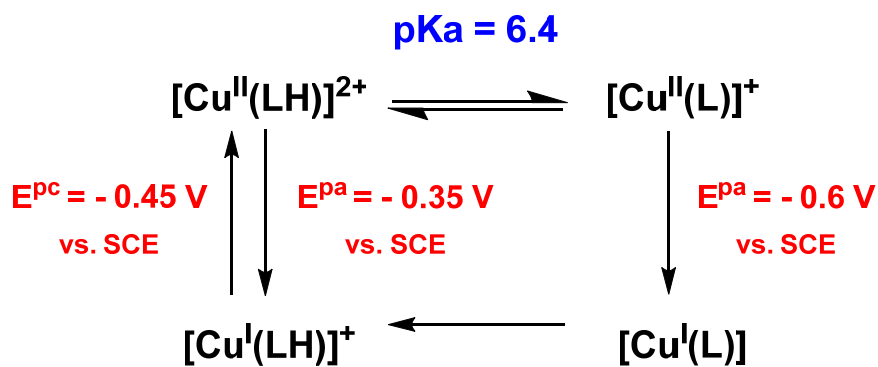


Figure S9. *Panel A.* Cyclic voltammograms of LH (red curve) and 2⁺ (blue: scanning towards positive and green: scanning towards negative potential values). *Panel B.* Cyclic voltammograms of 2⁺ as a function of the scan rate (from light blue to red: 10, 20, 50, 100, 200 and 500 mV.s⁻¹). [L] = 1.0 mM, [Cu(II)] = 0.9 mM, [phosphate buffer] = 100 mM at pH 7.1. The scan rate is 0.1 V.s⁻¹. Saturated Calomel Electrode was used as a reference.

The dependence of the cyclic voltammograms as a function of the scan rate can be explained by the following square-scheme mechanism:



Monitoring of ROS formation

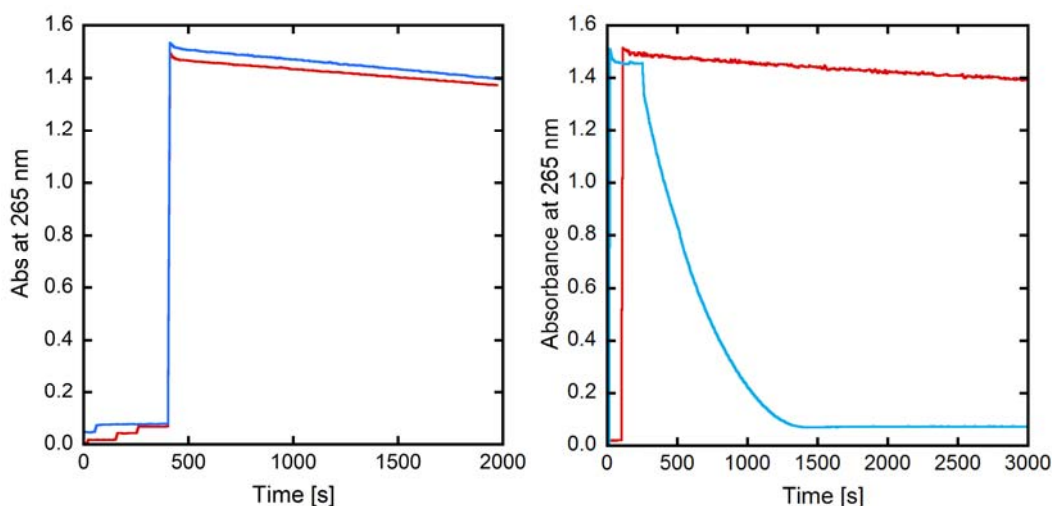


Figure S10. Left: Kinetics of ascorbate consumption, followed by UV-visible spectroscopy at 265 nm with subtraction of the background signal at 800 nm. A β 40 + Cu(II) + LH + Asc (red curve), A β 40 + Cu(II) + $\underline{1}^+$ + Asc (blue curve). Right: control experiments, corresponding to Asc only (red curve) A β 40 + Cu(II) + LH + Asc (light blue curve). [A β 40] = [LH] = [$\underline{1}^+$] = 12 μ M, [Cu(II)] = 10 μ M, [HEPES] = 100 mM, [Asc] = 100 μ M, T = 25°C, pH = 7.1.

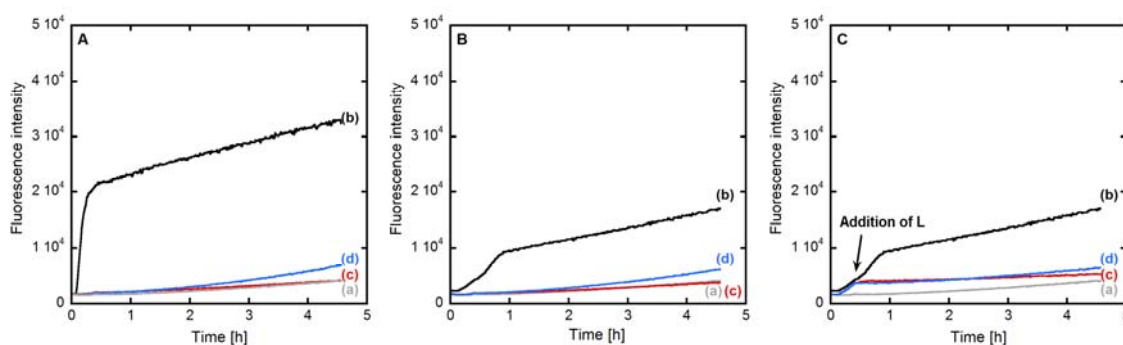


Figure S11. ROS production followed by 7-OH-CCA fluorescence. *Panel A.* a) Asc, b) Cu(II)+ Asc, c) $\underline{2}^+$ + Asc, d) $\underline{1}^+$ + Cu(II) + Asc. *Panel B.* a) Asc, b) A β 16 + Cu(II) + Asc, c) A β 16 + Cu(II) + LH + Asc, d) A β 16 + Cu(II)+ $\underline{1}^+$ + Asc. *Panel C.* a) Asc, b) A β 16 + Cu(II) + Asc, c) A β 16 + Cu(II) + Asc + LH, d) A β 16 + Cu(II) + Asc + $\underline{1}^+$ at 20 min. Asc was added 5 min after the beginning of the measurement. [A β 16] = [LH] = [$\underline{1}^+$] = 12 μ M, [Cu(II)] = 10 μ M, [CCA] = 500 μ M, [Asc] = 500 μ M, [phosphate buffer] = 50 mM, pH 7.1. Note that in presence of peptide, the maximum fluorescence is weaker due to the ability of the peptide to grasp the generated HO $^\circ$.^[3]

TEM images

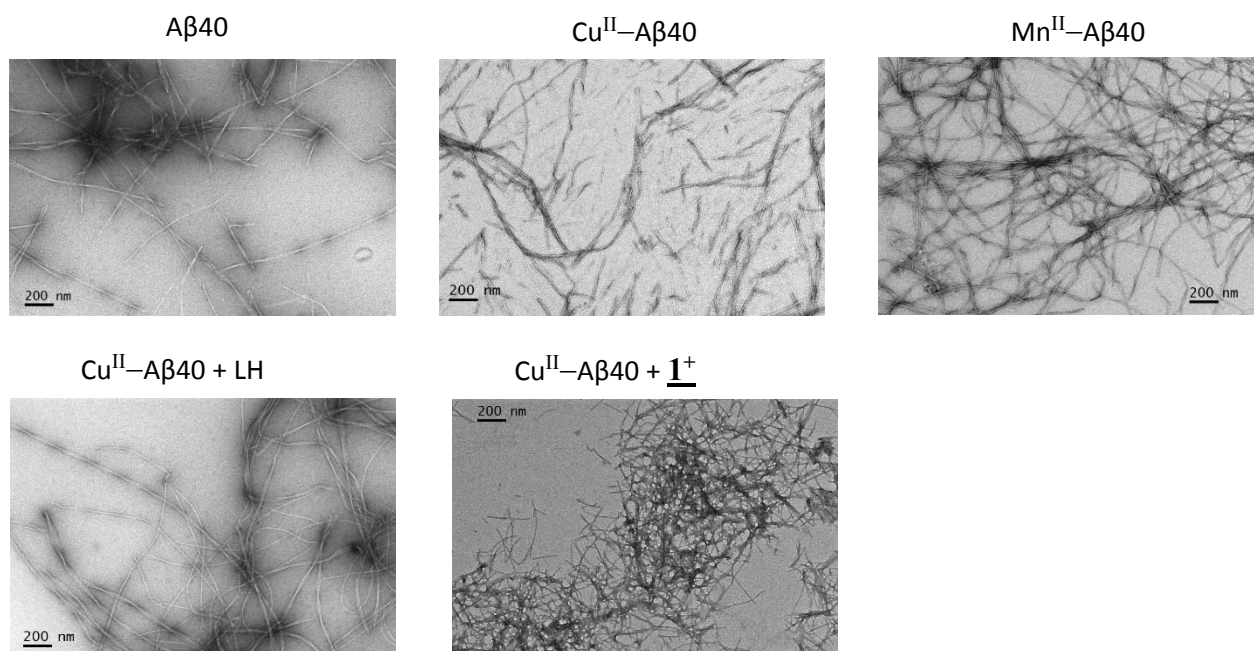


Figure S12. TEM images. The contrast agent is uranyl acetate (1%).

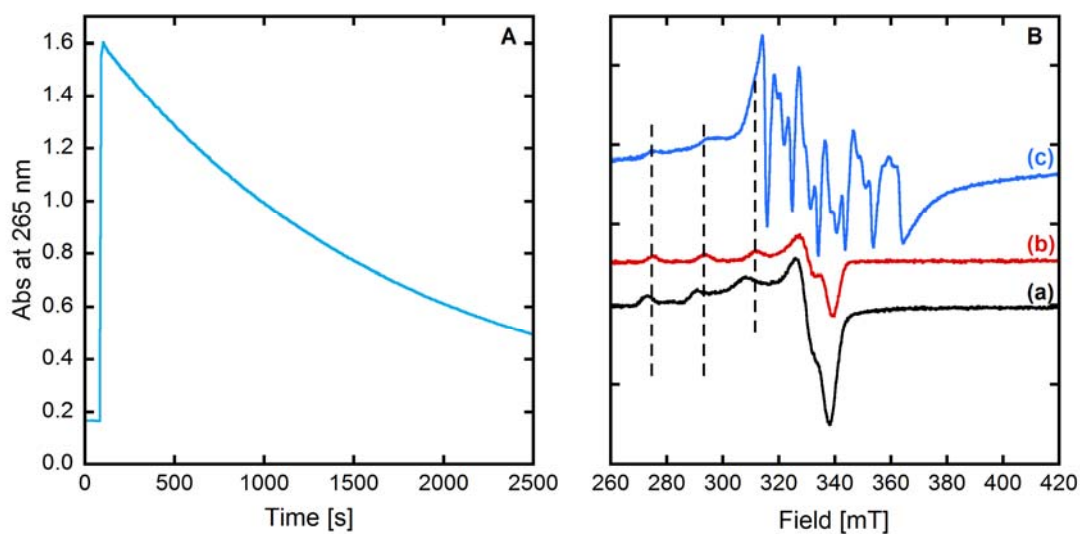


Figure S13. Panel A. Kinetics of ascorbate consumption, followed by UV-visible spectroscopy at 265 nm with subtraction of the background signal at 800 nm. IPG + Cu(II) + Asc. [IPG] = 24 μ M, [Cu(II)] = 10 μ M, [Asc] = 100 μ M, [HEPES] = 100 mM, T = 25°C, pH = 7.1. Panel B. EPR signatures of a) Cu(Aβ16), b) Cu(IPG), c) Cu(Aβ16) + Mn(IPG). [IPG] = [Mn(IPG)] = 400 μ M, [Aβ16] = 200 μ M, [⁶⁵Cu(II)] = 190 μ M, [Asc] = 100 μ M, [HEPES] = 50 mM, pH = 7.1. 10 % of glycerol was used as cryoprotectant.

Material et methods.

Chemicals. Reagents, except the ligands LH and L₂,^[1] were commercially available and were used as received. All the solutions were prepared in milliQ water (resistance: 18.2 MΩ.cm).

The Cu(II) ion source MnSO₄ was CuSO₄.5H₂O and the Mn(II) ion source was bought from Sigma-Aldrich.

HEPES buffer (sodium salt of 2-[4-(2-hydroxyethyl)piperazin-1-yl]ethanesulfonic acid) was bought from Sigma-Aldrich. A stock solution was prepared at 500 mM, pH = 7.1. Phosphate buffer was bought from Sigma-Aldrich. Two stock solutions, K₂HPO₄ and KH₂PO₄, were prepared at 500 mM, and they were mixed until to reach a stock solution at pH = 7.1.

Sodium ascorbate was bought from Sigma-Aldrich. A stock solution was prepared at 5 mM each day because of the quick degradation of the ascorbate.

Coumarin-3-carboxylic acid (CCA) was bought from Acros Organics. A stock solution at 5 mM was prepared in phosphate buffer at 500 mM, pH = 7.1. The stock solution was stored at 4°C.

ThT was bought from Acros Organics. A stock solution of at 250 μM was prepared in water without any further purification.

Synthesis of [Cu(LH)]²⁺, crystal's growing

NEt₃ (7.5 mg, 10μL, 0.075mM, 0.5 eq) was added to a solution of the ligand LH, synthesized as previously described^[4] (53.1 mg, 0.15mM, 1 eq) in absolute ethanol (2mL). A solution of Cu(NO₃)₂.6H₂O (36 mg, 0.15mM, 1 eq) in ethanol (1 ml) was added to this mixture and the solution was heated to 50°C for 30 min. A solution of NH₄PF₆ (49 mg, 0.3 mM, 2 eq) in ethanol (2mL) was then added and the resulting precipitate was isolated by filtration. The powder could be recrystallized from a solution of CH₃OH and CH₃CN by slow diffusion of CH₃COOEt.

Peptide. Aβ16 (DAEFRHDSGYEVHHQK) was bought from Genecust with purity grade > 95%. A stock solution was prepared at around 10 mM and stored at 4°C until used. Peptide concentration was determined by UV-visible absorption of Tyr10 considered as free tyrosine (at pH 2, (ε₂₇₆-ε₂₉₆) = 1410 M⁻¹cm⁻¹). Aβ40 (DAEFRHDSGYEVHHQKLVFFAEDVGSNKGAIIGLMVGGVV) was bought from Genecust with purity grade > 95%. Stock solution of the Aβ40 peptide was prepared by dissolving the powder in 100mM Tris buffer with 6 M of guanidinium chloride at approx. 800 μM. After an overnight incubation, the peptide was injected on a Superdex 75 column for further purification by FPLC. 15 mM NaOH and 150 mM NaCl elutant is used, at 0.8 mL.min⁻¹ flow rate. The peptide is detected at 293 nm and at a retention time of approx. 10 min. All the fractions corresponding to the peptide are collected. Peptide concentrations are then determined by UV-visible absorption of Tyr10 considered as free tyrosine (at pH 13, (ε₂₉₆-ε₃₆₀) = 2400 M⁻¹cm⁻¹). Aβ16 was used as an appropriate model for the binding site of the Aβ40 when high solubility was required (i.e. in EPR and electrochemistry).

DAHK was bought from Genecust with purity grade > 95% and dissolved in milli Q water to ~ 70 mM. The concentration was determined by UV-Vis, using a titrating Cu(II) solution of known concentration and following the absorbance of the d-d band of Cu(DAHK) complex formed.

X-ray diffraction study.

X-ray diffraction data for compound [Cu(LH)](PF₆)(NO₃) were collected by using a Kappa X8 APPEX II CCD Bruker diffractometer with graphite-monochromated MoK α radiation. Crystal was mounted on a CryoLoop (Hampton Research) with Paratone-N (Hampton Research) as cryoprotectant and then flashfrozen in a nitrogen-gas stream at 100 K. For compounds, the temperature of the crystal was maintained at the selected value (100K) by means of a 700 series Cryostream cooling device to within an accuracy of ± 1 K. The data were corrected for Lorentz polarization, and absorption effects. The structures were solved by direct methods using SHELXS-97⁶ and refined against F^2 by full-matrix least-squares techniques using SHELXL-2017⁷ with anisotropic displacement parameters for all non-hydrogen atoms. Hydrogen atoms were located on a difference Fourier map and introduced into the calculations as a riding model with isotropic thermal parameters. All calculations were performed by using the Crystal Structure crystallographic software package WINGX.⁸⁻⁹

The crystal data collection and refinement parameters are given in Table S1.

CCDC 1578865 contains the supplementary crystallographic data for this paper. These data can be obtained free of charge from the Cambridge Crystallographic Data Centre via <http://www.ccdc.cam.ac.uk/Community/Requestastructure>.

Electron Paramagnetic Resonance. Electron Paramagnetic Resonance (EPR) data were recorded using an Elexsys E 500 Bruker spectrometer, operating at a microwave frequency of approximately 9.5 GHz. Spectra were recorded using a microwave power of 20 mW across a sweep width of 150 mT (centered at 310 mT) with modulation amplitude of 0.5 mT. Experiments were carried out at 110 K using a liquid nitrogen cryostat. EPR samples were prepared from stock solution of ligand diluted down to 0.2 mM in H₂O. 0.9 eq. of ⁶⁵Cu(II) was added from 25 mM ⁶⁵Cu(NO₃)₂ stock solution home-made from a ⁶⁵Cu foil. If necessary, pH was adjusted with H₂SO₄ and NaOH solutions. Samples were frozen in quartz tube after addition of 10% glycerol as a cryoprotectant and stored in liquid nitrogen until used.

Parallel spin Hamiltonian parameters were obtained directly from the experimental spectra and were calculated from the second and the third hyperfine lines in order to remove second-order effects.

UV-Vis spectrophotometry. Affinity and pKa measurements were recorded on a spectrophotometer Agilent 8453 at 25°C in 1 cm path length quartz cuvette. The pH was adjusted using H₂SO₄ and NaOH.

Electrochemistry. Cyclic voltamograms were recorded on a Autolab PGSTAT302N at 25°C. Saturated Calomel Electrode was used as a reference, Platine electrode as the counter electrode and a glassy carbon electrode as the working electrode. The working electrode was carefully polished before each measurement on a red disk NAP with 1 µm AP-A suspension under abundant distillate water flow during at least three minutes (Struers). The solution was deoxygenated by bubbling Argon before each measurement. No additional supporting electrolyte was required because of the high concentration of phosphate buffer in the solution. The scanning rate was 0.1 V.s⁻¹. The samples were prepared from stock solutions of ligand and Cu(II) down to approx. 0.2 mM in a buffered solution. pH was adjusted with H₂SO₄ and NaOH solutions.

ROS formation. UV-vis kinetics were recorded on a spectrophotometer Agilent 8453 at 25°C in 1 cm path length quartz cuvette, with an 800 rpm stirring. The samples were prepared from stock solutions of ligand/complex, peptide Aβ40 and Cu(II) diluted down to 12, 12 and 10 µM respectively in HEPES solution, pH = 7.1. Ascorbate is diluted down to 100 µM.

CCA experiments were recorded on a FLUOstar OPTIMA BMG LABTECH at 25°C in a 96-well plate bought from Dutscher SAS. CCA was excited at 390 nm and the fluorescence was recorded at 450 nm. The gain was 1350. The samples were prepared from stock solutions of ligand, peptide and Cu(II) diluted down to 12, 12 and 10 µM respectively in phosphate solution, pH = 7.1. CCA was added at a resulting concentration of 500 µM. Injector was used for the addition of ascorbate diluted down to 500 µM, 5 min after the beginning of the experiment.

ThT experiments were recorded on a FLUOstar OPTIMA BMG LABTECH at 37°C in a 384-well plate bought from Dutscher SAS. ThT was excited at 440 nm and the fluorescence was recorded at 490 nm. The gain was 1200. The samples were prepared from stock solutions of ligand/complex, peptide and Cu(II) diluted down to 20, 20 and 18 µM respectively in HEPES buffer, pH = 7.1. ThT was added at a resulting concentration of 10 µM.

Transmission electron microscopy. Specimens were prepared for electron microscopy using the conventional negative staining procedure. 20 µL of solution was absorbed on Formvar-carbon-coated grids for 2 min, blotted, and negatively stained with uranyl acetate (1%) for 1 min. Grids were examined with a TEM (Jeol JEM-1400, JEOL Inc, Peabody, MA, USA) at 80 kV. Images were acquired using a digital camera (Gatan Orius, Gatan Inc, Pleasanton, CA, USA) at a x 25 000 magnification.

References.

- [1] S. Noël, F. Perez, S. Ladeira, S. Sayen, E. Guillon, E. Gras and C. Hureau, *J. Inorg. Biochem.* **2012**, *117*, 322-325.
- [2] C. Policar, S. Durot, F. Lambert, M. Cesario, F. Ramiandrasoa and I. Morgenstern-Badarau, *Eur. J. Inorg. Chem.* **2001**, 1807-1818.
- [3] C. Cheignon, F. Collin, P. Faller and C. Hureau, *Dalton Transactions* **2016**, *45*, 12627-12631.
- [4] F. Cisnetti, A. S. Lefevre, R. Guillot, F. Lambert, G. Blain, E. Anxolabéhère-Mallart and C. Policar, *Eur. J. Inorg. Chem.* **2007**, 4472-4480.
- [6] Sheldrick, G. M. SHELXS-97, Program for Crystal Structure Solution, University of Göttingen, Göttingen, Germany, **1997**.
- [7] G. M. Sheldrick, *Acta Crystallogr., Sect. A: Found. Crystallogr.*, **2008**, *64*, 112-122
- [8] Farrugia, L. J. *J. Appl. Cryst.*, **1999**, *32*, 837.
- [9] G. Bernardinelli and H. D. Flack, *Acta Crystallogr., Sect. A: Found. Crystallogr.*, **1985**, *41*, 500-511.